RSC Advances

PAPER

View Article Online
View Journal | View Issue

Cite this: *RSC Adv.*, 2023, **13**, 5900

One-step potentiostatic electrodeposition of NiS–NiS_2 on sludge-based biochar and its application for a non-enzymatic glucose sensor†

Suxing Luo, *[a] Meizhi Yang,[b] Jiang Li [c] and Yuanhui Wu *[a]

Received 13th December 2022
Accepted 7th February 2023

DOI: 10.1039/d2ra07950j

rsc.li/rsc-advances

Conventional nanomaterials are available in electrochemical glucose nonenzymatic sensing, but their broad applications are limited due to their high cost and complicated preparation procedures. In this study, NiS–NiS_2/sludge-based biochar/GCE was fabricated by one-step potentiostatic electrodeposition on biochar and used as an interface material for non-enzymatic sensing of glucose in 0.1 M NaOH. With an electrodeposition time of 300 s, the as-prepared sensors delivered the best electrochemical performance toward glucose due to the synergistic effects of NiS–NiS_2 and sludge-based biochar. The as prepared NiS–NiS_2/sludge-based biochar surface morphology, surface composition, and electrochemical properties were characterized by SEM elemental mapping, XPS and cyclic voltammetry. Under optimized conditions, the linearity between the current response and the glucose concentration has been obtained in the range of 5–1500 μM with a detection limit of 1.5 μM. More importantly, the fabricated sensor was successfully utilized to measure glucose in serum of sweetened beverages and human blood. Accordingly, NiS–NiS_2/sludge-based biochar/GCE can hopefully be applied as a normal enzyme-free glucose sensor with excellent properties of sensitivity, reproducibility, stability, as well as sustainability.

1 Introduction

Efficient and reliable determination of blood glucose is the key guarantee for prevention and observation of diabetes promptly.[1,2] For traditional glucose detection, enzymatic glucose sensors have been used most widely because of their highly selectivity, simplicity, and reliability.[3,4] However, the storage and use of enzymatic glucose sensors have conditional limits due to instability of enzymes, intolerance of pH and temperature variation, also including its high cost.[5,6] Hence, it is required to design a more convenient non-enzymatic glucose sensing device with sensors.

Recently, non-enzymatic glucose sensors including noble metallic materials (Au, Pt, and Pd) and their alloys were developed extensively due to noble metal having lower electron transfer resistance and higher electro-catalytic activities.[5,7,8] However, the high cost of noble metals sensor is bounded to be limited in practical applications.[9] As reported up to now, nickel-based compounds including sulfides, hydroxides, oxides, and phosphates have been reported as efficient glucose sensors materials, of which nickel sulfides exhibited excellent electro-catalytic performance and electrical conductivity, and nickel sulfides have been sufficiently exploited in the progress of enzyme mimic glucose sensors, such as Ni_3S_2/carbon nanotube, NiS/$Ni(OH)_2$/NH_4PA/PPyNTs, NiS/S-g-C_3N_4.[5,6,10–13] These sensors could detect glucose sensitively, but expensive carbonaceous materials (C_3N_4, PPyNTs, carbon nanotube) yet increase the test cost.[6,14] With regards to this situation, it is necessary to fabricate a novel electrochemical sensor that not only requires high analytical efficiency and sensitivity but also utilizes low-cost and sustainable materials.

In this study, we proposed using excess sludge as the raw material for glucose sensor. As a major residue of municipal sewage treatment plant, excess sludge is regarded as its major pollutant and usually treated with simple landfills, fertilization, incineration, *etc.* Without further treatment, it could cause secondary pollution easily.[15,16] However, its abundant organic matter and surface adsorption sites enable excess sludge with potential for biochar preparation. So far, the application of biochar as an electrode modifier, aiming at determinations of inorganic ions and organic species, has gained noticeable popularity and recognition due to its rich pore structures and functional groups.[17–20]

Here, by integrating sludge-based biochar with nickel sulfides, a novel enzyme-free electrochemical glucose sensor has been developed. Nickel sulfides were *in situ*

[a]*Department of Chemistry and Chemical Engineering, Zunyi Normal College, Zunyi, 563006, P. R. China. E-mail: suxingluo@126.com; yhwull@126.com*
[b]*Guizhou Open University, Guiyang, 550023, P. R. China*
[c]*College of Chemistry and Chemical Engineering, Shanxi Datong University, Datong, 037009, P. R. China*

† Electronic supplementary information (ESI) available. See DOI: https://doi.org/10.1039/d2ra07950j

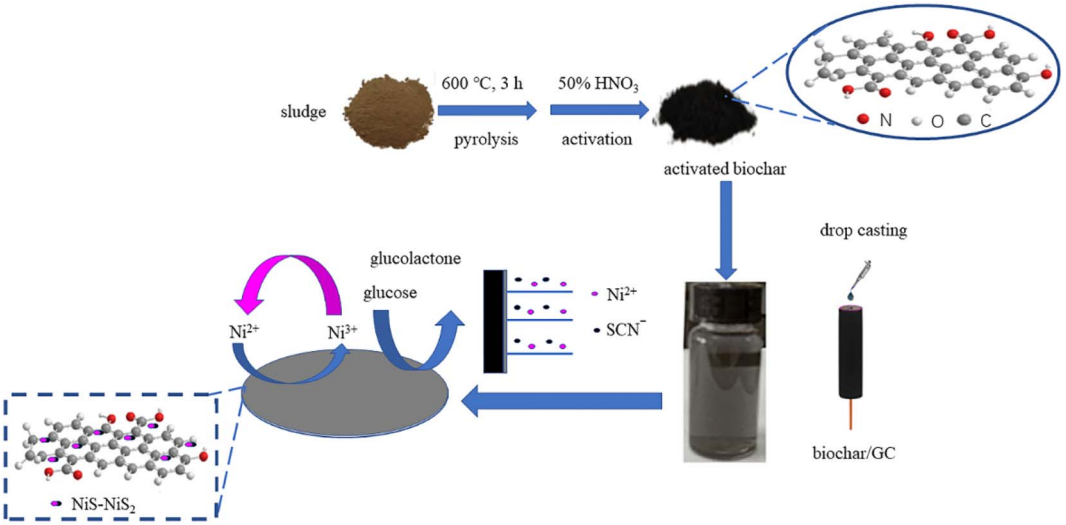

Scheme 1 Schematic diagram for the fabrication of NiS–NiS_2/sludge-based biochar/GCE and sensing of glucose by an electrochemical strategy.

electrodeposited on the surface of sludge-based biochar due to electrodeposition having significant advantages of relatively low cost, easy operation, and well condition controlling.[21,22] Consequently, the NiS–NiS_2/sludge-based biochar/GCE was constructed (Scheme 1). This proposed sensor was low-cost, eco-friendly, sensitive and convenient. In addition, this electrochemical method was successfully applied to determine glucose effectively in real sweetened beverages and human blood samples.

2 Experimental section

2.1 Chemicals and reagents

The excess sludge sampled from the Gaoqiao Wastewater Treatment Plant in Zunyi, China, was used as the raw material for biochar synthesis. Chemicals such as nickel nitrate hexahydrate, potassium thiocyanide and glucose were purchased from Aladdin Industrial Corporation (Ontario, CA, USA) and used without further treatment.

2.2 Preparation of sludge-based biochar

To prepare sludge-based biochar, excess sludge was firstly transferred to an Ultrasonic Cell Crusher with 600 W for 20 min, then dried overnight at 105 °C. Subsequently, the excess sludge was screened with 100 mesh sieve (0.15 mm) and pyrolyzed at 600 °C [23] in tubular reactor for 4 h under argon protection with heating rate 5 °C min^{-1}. After that, the product immersed in 0.5 M HF and evaporated at 100 °C to remove ashes.[24] Finally, the residual solid product was rinsed several times with distilled water until the pH of suspension was neutral and then dried at 105 °C to obtain sludge-based biochar.

2.3 Activation of sludge-based biochar

To increase surface functional groups for further modification, the sludge-based biochar was activated by nitric acid (HNO_3). For the activation, 25 mL 50% (v/v) nitric acid was added to 0.2 g sludge-based biochar. Then the mixture was transferred into a reflux system under constant stirring at 60 °C for 3 hours, and then washed to pH neutral and dried.

2.4 Fabrication of the modified electrodes

Prior to use, a glassy carbon electrode (GCE) was mirror polished with 0.3 μM and 0.05 μM alumina slurries on an abrasive paper, and then dipped in alcohol after being sonicated in deionized water. Firstly, activated sludge-based biochar was ultrasonically dispersed in an aqueous solution to obtain 1 mg mL^{-1} activated biochar suspension. Then, 7 μL of 1 mg mL^{-1} activated biochar suspension was carefully transferred onto the mirror-like surface of the GCE dried at room temperature for obtaining sludge-based biochar/GCE. Thirdly, the modified electrodes were fabricated by directly electrodepositing NiS–NiS_2 on sludge-based biochar/GCE *via* a potentiostatic method in electrolyte of 0.05 M $NiSO_4$ and 0.2 M KSCN at a voltage of −0.8 V and certain time (210 s, 300 s, 420 s), which were labeled as Ni-B-210, Ni-B-300, and Ni-B-420, respectively.

2.5 Characterization measurements

The surface morphologies and the elemental mapping of the as-prepared modified electrodes were performed by scanning electron microscope (SEM, TESCAN MIRA LMS, Czech Republic) operated at an accelerating voltage of 15 kV. The surface composition of the modified electrodes was captured by X-ray photoelectron spectroscopy (XPS, Thermo Scientific) using Al-Kα exciting radiation (1486.6 eV, 450 W). The passing energy and energy step size for high-resolution spectra were 50 eV and 0.1 eV, respectively. And all high-resolution spectra were corrected with the adventitious C 1s peak (284.8 eV).

2.6 Electrochemical measurements

The NiS–NiS_2/sludge-based biochar/GCE electrodes were evaluated as a glucose sensor in 0.1 M NaOH. All electrochemical experiments were carried out using a 2273 electrochemical system (Princeton Applied Research PARSTAT2273 Electrochemical Workstation), consisting of a typical three-electrode cell equipped with the NiS–NiS_2/sludge-based biochar/GCE electrode as the working electrode, a platinum wire and an Ag/AgCl electrode, which serves as the auxiliary and reference electrodes, respectively.

3 Results and discussion

3.1 Morphological characterization

In order to monitor the morphology and composition of electrodeposited products, different electrodeposition time was studied. The morphologies of the as-prepared modified electrodes at three different electrodeposition time were investigated and compared in Fig. 1. The sludge-based biochar/GCE has rough surface with layered porous structure (Fig. S1†). After electrodeposition, large quantities of asymmetric small clusters (0.1–5 μm, almost below 1 μm) appeared on all three kinds of modified electrodes, and all of them can barely observe the morphology of original sludge-based biochar/GCE as small clusters almost covering the whole surface (Fig. S1†). Noticeably, the average diameter of electrochemically deposited particles was reduced gradually as the increasing of deposition time.

To measure elemental content of the electrodeposited products, the as-prepared modified electrodes with different electrodeposition time were characterized by element mapping analysis and the results were shown in Fig. S2.† It was found that both of the Ni and S element were successfully electrodeposited on surface of all electrodes. And the atomic ratios of Ni to S of Ni-B-210, Ni-B-300, and Ni-B-420 were 80.1 : 19.9, 53.9 : 46.1, and 28.7 : 71.3, respectively. Correspondingly, the main possible products on the electrodes discussed above were $Ni(OH)_2$–NiS_2/sludge-based biochar/GCE, NiS–NiS_2/sludge-based biochar/GCE, NiS_2 sludge-based biochar/GCE, respectively. In addition, these compounds information on the electrodes were verified in Section 3.2.

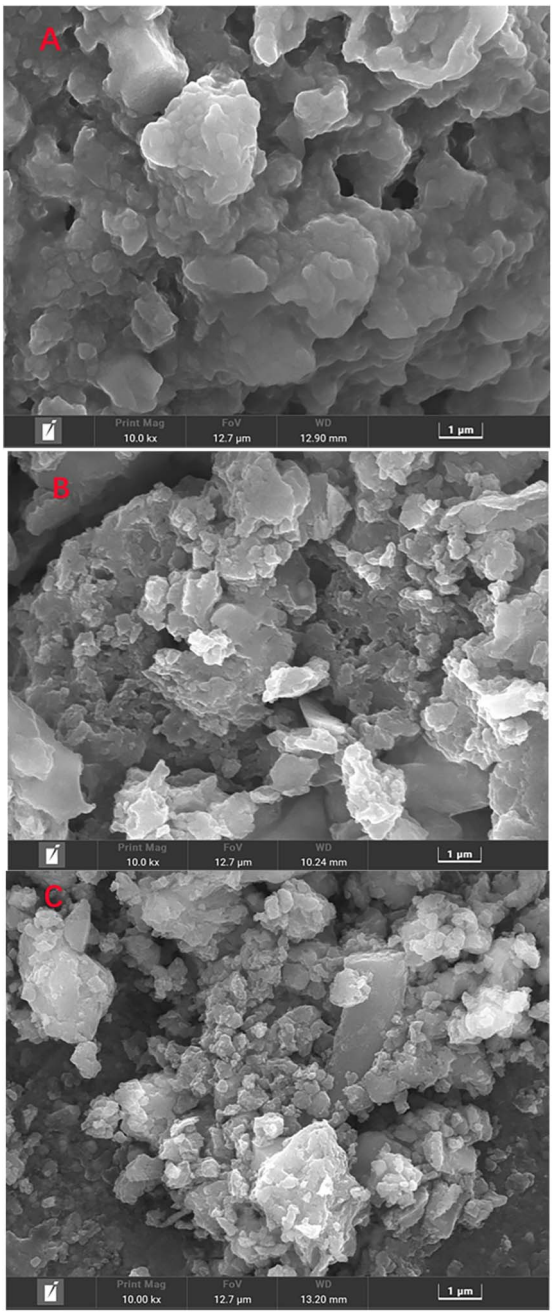

Fig. 1 SEM images of as-prepared modified electrodes obtained at different electrodeposition time: (A) 210 S, (B) 300 S, (C) 420 S.

3.2 X-ray photoelectron spectra (XPS) studies

Furthermore, XPS high resolution spectra were used to gain chemical states and compound information on the surface of three kinds of as-prepared modified electrodes with different electrodeposition time were displayed in Fig. 2. Fig. 2A displayed the Ni $2p_{3/2}$ spectrum of Ni-B-210. The binding energies at 855.9 eV and 861.7 eV were indexed to NiS_2 and $Ni(OH)_2$, respectively.[7,25] The main peak of the Ni $2p_{3/2}$ was fitted with two peaks at 853.4 eV and 856.0 eV in Fig. 2C were assigned to NiS and NiS_2.[26] In Fig. 2E, the characteristic peak for NiS_2 at binding energy of 856.0 eV was observed. The peaks of S $2p_{3/2}$ at 162.8 eV can be attributed to S^{2-} or S^{-} in the as-electrodeposited samples while only S $2p_{3/2}$ of Ni-B-300 showed slight oxidation, mainly resulting from NiS oxidation product, spices SO_4^{2-}.[27,28] Above all, XPS data results were in agreement with the element mapping results.

3.3 Electrochemical behaviors of the three kinds of modified electrodes toward NaOH and glucose

Cyclic voltammetry (CV) was used to investigate the different electrochemical behaviors of the as-prepared modified electrodes at different electrodeposition time in 0.1 M NaOH without or with 0.5 mM glucose. As shown in Fig. 3, the NiS–NiS_2/sludge-based biochar/GCE exhibited excellent electrocatalytic performance toward glucose comparing with the other

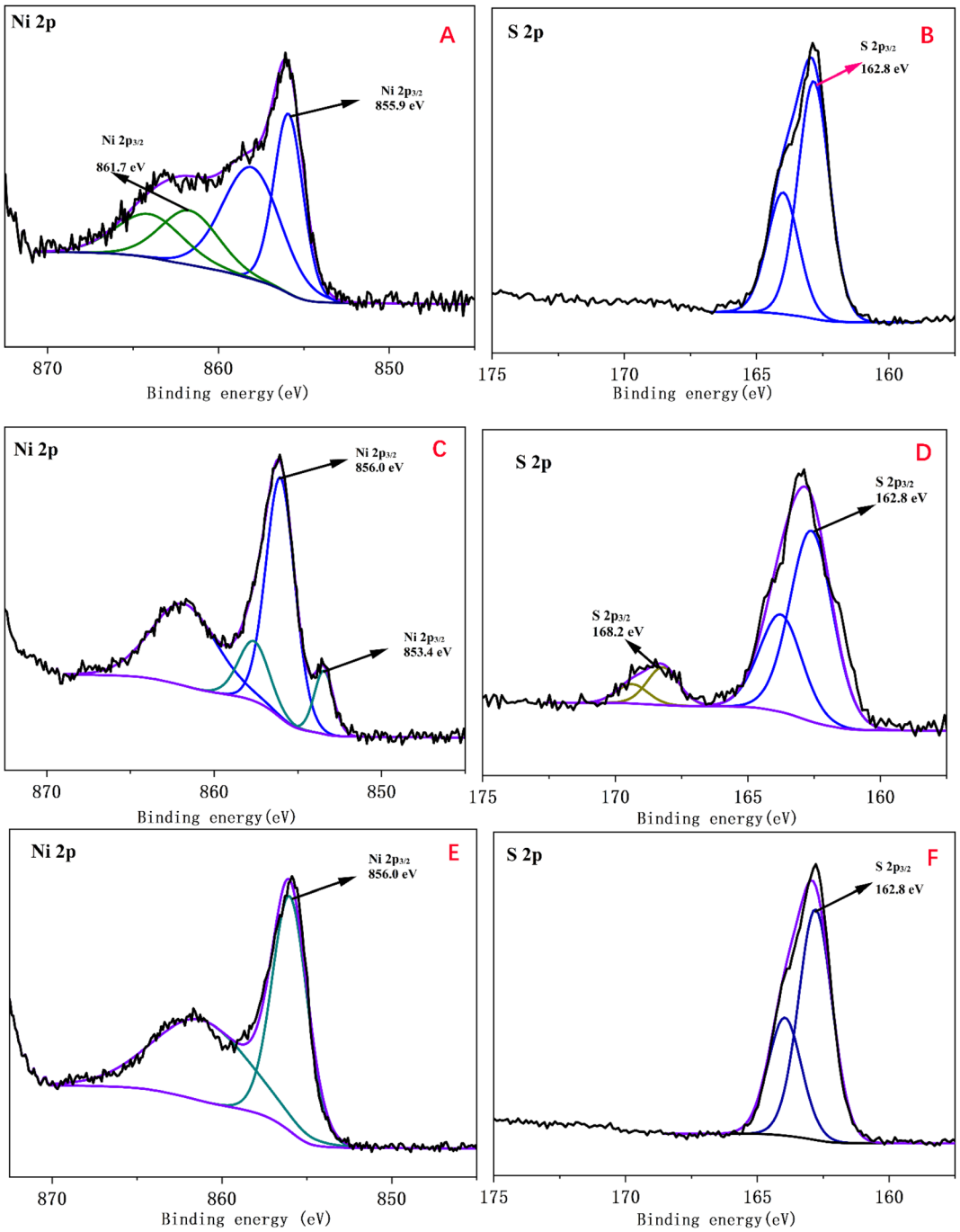

Fig. 2 High resolution XPS spectrum of (A) Ni 2p (B) S 2p of $Ni(OH)_2$–NiS_2/sludge-based biochar/GCE, (C) Ni 2p (D) S 2p of NiS–NiS_2/sludge-based biochar/GCE, (E) Ni 2p (F) S 2p of NiS_2 sludge-based/biochar/GCE.

two electrodes, suggesting NiS performed best electrochemical activity comparing with $Ni(OH)_2$ and NiS_2. A pair of redox peaks of NiS–NiS_2/sludge-based biochar/GCE in 0.1 M NaOH at 0.55 V (*vs.* AgCl) and 0.36 V (*vs.* AgCl) correspond to the transformation of NiS, NiS_2 (Ni(II)) to NiSOH and NiS_2OH (Ni(III)), and then reduction behavior of NiSOH, NiS_2OH to NiS and NiS_2, respectively[14,29] (eqn (1)).

$$\begin{aligned} NiS + OH &\rightleftharpoons NiSOH + e^- \\ NiS_2 + OH^- &\rightleftharpoons NiS_2OH + e^- \end{aligned} \quad (1)$$

After the addition of 0.5 mM glucose, the oxidation potential appeared at 0.50 V, related to the electrocatalytic oxidation of glucose occurring on NiS–NiS_2/sludge-based biochar/GCE, corresponding to the reaction equation as follow:

$$\begin{aligned} NiSOH + \text{glucose} &\rightleftharpoons NiS + \text{glucolactone} \\ NiS_2OH + \text{glucose} &\rightleftharpoons NiS_2 + \text{glucolactone} \end{aligned} \quad (2)$$

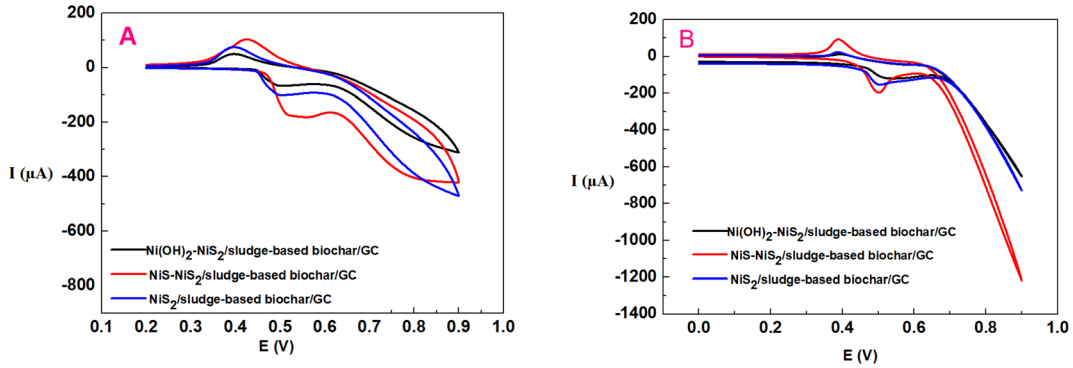

Fig. 3 Cyclic voltammograms of $Ni(OH)_2$–NiS_2/sludge-based biochar/GCE, NiS–NiS_2/sludge-based biochar/GCE, and NiS_2 sludge-based/biochar/GCE in 0.1 M NaOH (A) in the absent of glucose; (B) in the present of 0.5 mM glucose.

3.4 Electrochemical behaviors of NiS–NiS_2/sludge-based biochar/GCE toward glucose

In order to verify the electrocatalytic performance of NiS–NiS_2/sludge-based biochar/GCE compared with the other electrodes, CV measurements were recorded in 0.1 M NaOH solution containing 0.5 mM glucose as shown in Fig. 4. First, the bare GCE and biochar/GCE did not show any appreciable electrocatalytic response. And then the poorly defined oxidation peaks were observed at NiS–NiS_2/GCE. At last, for NiS–NiS_2/sludge-based biochar/GCE, the oxidation peak current increased significantly and the oxidation peak potential decreased obviously compared with NiS–NiS_2/GCE. This clearly indicates that the NiS–NiS_2/sludge-based biochar/GCE had excellent electrocatalytic performance towards the electro-oxidation of glucose.

The high response current of NiS–NiS_2/sludge-based biochar/GCE for detecting glucose was mainly caused by the synergistic effects of NiS–NiS_2 and sludge-based biochar. On the one hand, unique porous structure as well as abundant functional groups of sludge-based biochar[30] provided strong adsorption capacity and abundant electrocatalytic active site for glucose detection. On the other hand, the high conductivity of NiS may further enhance its electrocatalytic performance in glucose analysis process.[6] In addition, the redox pair (Ni(II)/Ni(III)) also can boost the electrocatalytic behavior of glucose as both electronic medium and catalyst.[31] Thus, the proposed electrochemical sensor, NiS–NiS_2/sludge-based biochar/GCE, is capable of being electrode material for building nonenzymatic glucose sensors with excellent electrocatalytic performance.

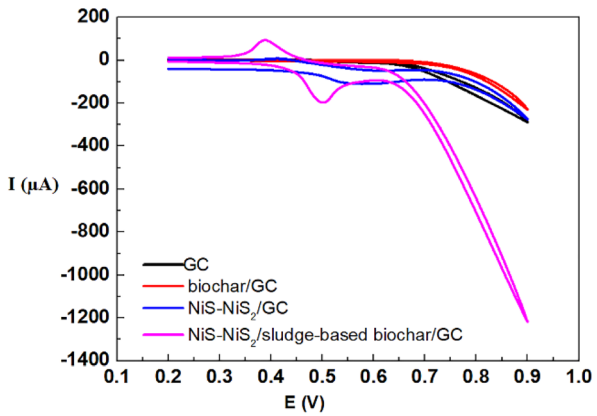

Fig. 4 Comparative cyclic voltammetry responses of bare GCE, sludge-based biochar/GCE, NiS–NiS_2/GCE, and NiS–NiS_2/sludge-based biochar/GCE were obtained for 0.5 mM glucose in 0.1 M NaOH solution.

The important rate-determining step of glucose electro-oxidation on NiS–NiS_2/sludge-based biochar/GCE was investigated by a series of CV tests at scan rates ranging from 20 to 200 mV s^{-1}. Fig. 5A and C depicted the CV curves of NiS–NiS_2/sludge-based biochar/GCE without or with 0.5 mM glucose in 0.1 M NaOH solution, respectively. After the addition of glucose, a pair of well-defined and enhanced oxidation peaks were clearly observed, which shifted to a little negative value comparing with that of Ni(II) oxidizing to Ni(III), owing to oxidization of glucose. These experiments demonstrated that NiS–NiS_2/sludge-based biochar/GCE showed excellent electrocatalytic activity towards glucose. As the scanning rates increasing, all anodic peak potential shifted positively while the cathodic peak potential moved negatively instead, indicating that the electrochemical reactions were quasi-reversible and there were kinetic limitations between the reaction sites of the modifier and substrate. Furthermore, both anodic and cathodic peak current enhanced linearly with the square root of scan rate from 20 to 200 mV s^{-1} (both Fig. 5B and D), indicating that the diffusion process of OH^- anions without glucose is the rate-determining step of NiSOH and NiS_2OH formation. Similarly, the redox reaction of glucose on NiS–NiS_2/sludge-based biochar/GCE was a typical diffusion controlled process. This indicates that the redox reaction occurring on the modified electrode is fast and reversible,[32] which is in consistent with formerly reported nickel compounds modified electrodes.[6,33]

3.5 Amperometric detection of glucose

To achieve amperometric measurements of glucose oxidation on NiS–NiS_2/sludge-based biochar/GCE, maximum current response was investigated at applied potentials (0.4 V, 0.5 V, 0.55 V and 0.6 V). The results showed that the current response improved as the applied potential increasing to 0.55 V, and

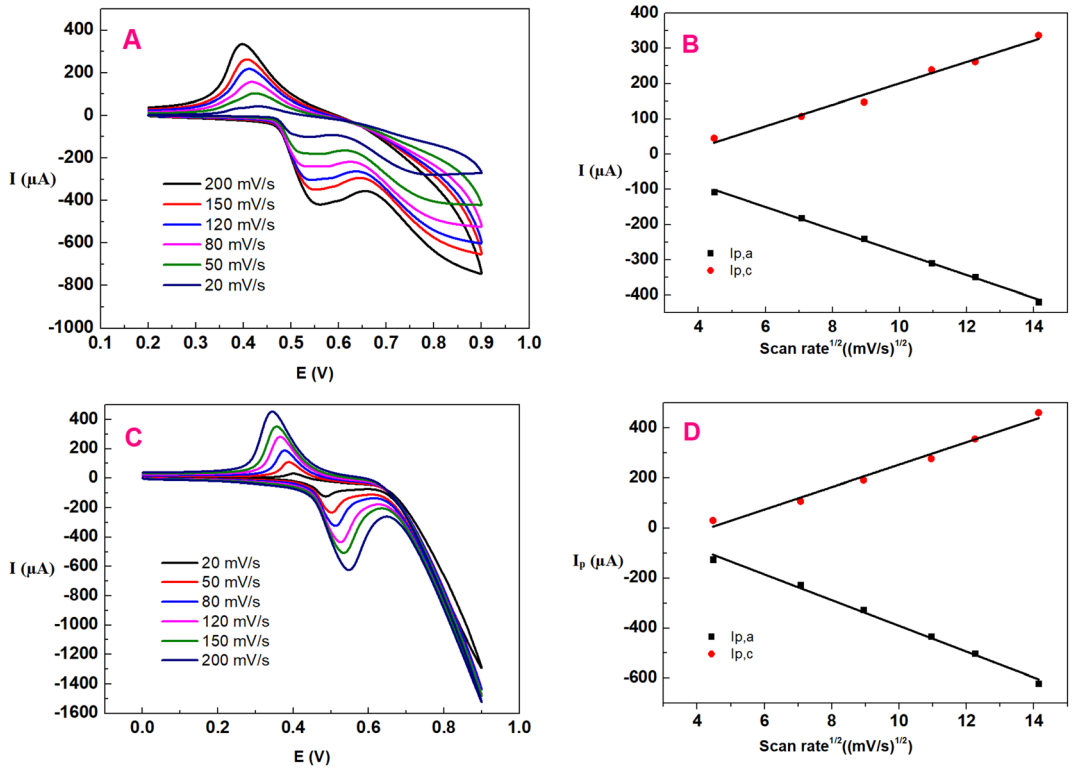

Fig. 5 CV curves of NiS– NiS_2/sludge-based biochar/GCE at different scan rates in 0.1 M NaOH solution without glucose (A) and with 0.5 mM glucose (C). The relationship between peak current and square root of the scan rate without glucose (B) and with 0.5 mM glucose (D).

subsequently began to fall afterwards. Consequently, 0.55 V was determined as the working potential for the amperometric glucose sensor. Furthermore, the real-time amperometric detection of glucose on the proposed sensor was investigated by consecutive injecting of glucose into the 0.1 M NaOH under constantly stirring, and the result was displayed in Fig. 6. Apparently, the continuous mass rising of glucose resulted in a stepwise growth of the current value and a steady state current achieved within 6 s, which suggested the fabricated sensor as a sensitive non enzymatic glucose sensor with favorable linear range from 5 to 1500 μM and the detection limit was calculated to be 1.5 μM.

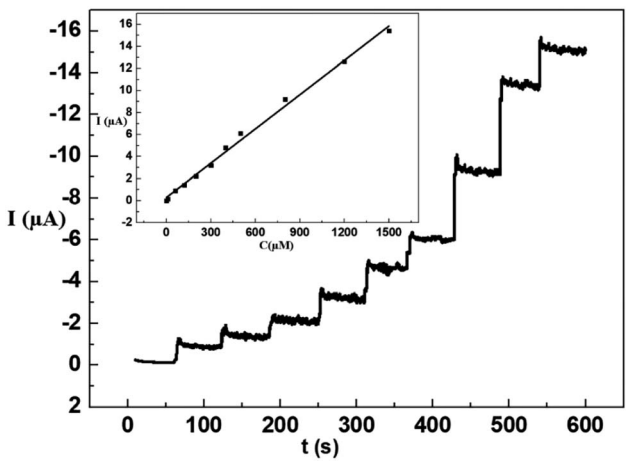

Fig. 6 The amperometric response of NiS–NiS_2/sludge-based biochar/GCE with successive addition of different amounts of glucose in 0.1 M NaOH (inset: calibration plot between current density *vs.* glucose concentration).

To verify the applicability of NiS–NiS_2/sludge-based biochar/GCE, various of different electrochemical nonenzymatic glucose sensors based on nickel sulfide were summarized in Table 1 to compare their scope of application. The fabricated electrode in our study showed comparably sensitivity when contrasted with other previous reports.

3.6 Selectivity, repeatability, reproducibility, and stability studies of NiS–NiS_2/sludge-based biochar/GCE

Above all, selectivity is one of the important characteristics in practical applications of sensor. Generally, the concentrations of interfering species were often selected at physiological level to test the selectivity of the sensor.[33] Thus, for the 0.5 mM glucose detection process, amperometric measurements were utilized to investigate the interferences including 60 μM ascorbic acid (AA), dopamine (DA), uric acid (UA), Cysteine (Cys), sodium chloride (NaCl), magnesium (Mg^{2+}), calcium (Ca^{2+}). The amperometric responses of the interference compounds above were given in Fig. S3.† Obviously, these interfering compounds had not noticeable effect on the determination of glucose, and the current response less than 5%. Secondly, the reproducibility of the method was examined by preparing four different NiS–NiS_2/sludge-based biochar/GCE

Table 1 Comparisons of various electrochemical non-enzymatic sensors based on nickel sulfide for glucose[a]

Type of the electrode	Method of modification electrode	Determination techniques	Linear range (μM)	Detection limit (μM)	Reference
NiS/S-g-C_3N_4	Drop casted on GCE	CV, LSV, Amp *I–t*	0.1–2100	1.5	6
NiS/$Ni(OH)_2$/NH_4PA/PPyNTs	Drop casted on GCE	CV	0–600	3.1	14
Hierarchical Ni_3S_2 electrode	Hydrothermal method	CV, EIS, Amp *I–t*	0.0005–3000	0.82	34
Ni_3S_2/carbon nanotube	Hydrothermal approach	CV, EIS, CA, Amp *I–t*	30–500	1	13
NiS/rGO nanohybrid	Drop casted on GCE	CV, LSV, Amp *I–t*	50–1700	10	35
Crystalline β-NiS	Atomic layer deposition method	CV, Amp *I–t*	0.005–60	1.2	36
3D Ni_3S_2 nanosheets/Ni foam	One-step hydrothermal approach	CV, EIS, CA, Amp *I–t*	0.005–3000	1.2	37
NiS– NiS_2/sludge-based biochar/GCE	Electrodeposition	Amp *I–t*	5–1500	1.5	This work

[a] CV – Cyclic voltammetry; Amp It – Amperometry; LSV-Linear sweep voltammetry; EIS – Electrochemical impedance spectroscopy; g-C_3N_4 – Graphitic carbon nitride; NH_4PA/PPyNTs – ammonium polyacrylate-functionalized polypyrrole nanotubes; rGO – reduced graphene oxide.

separately and checked their glucose response (10 μM) parallelly. The RSD of four electrodes was 4.8%, indicating the electrode fabrication and the glucose detection procedure were highly reproducible. Then, the stability of NiS–NiS_2/sludge-based biochar/GCE was also investigated after keeping in air at room temperature for 7 days, the peak current of glucose was reduced about 4.7% and the oxidation peak potential remained unchanged. Finally, the electrochemical responses (CV and amperometric) at 0.5 mM glucose were studied by four modified electrodes. After 5 parallel tests, the RSD value was 4.2%, showing that the sensor has great reproducibility. In summary, NiS–NiS_2/sludge-based biochar/GCE has excellent performs on glucose detection in experiment conditions.

3.7 Real sample analysis

In order to further estimate the sensor's practicability, the NiS–NiS_2/sludge-based biochar/GCE was utilized to determine glucose in human blood sample and oral glucose liquid, respectively. The blood sample was provided by one of the authors and used without further treatment. Before the test, the glucose oral liquid was diluted by dissolving 1 mL into 50 mL deionized water. The electrode was first calculated by adding glucose three times, then, the blood sample and oral glucose liquid were successively added into 100 mL 0.1 M NaOH solution, and amperometric detection was performed at 0.55 V working potential, and calculation results shown in Table 2.

Table 2 Determination of glucose in blood and glucose oral liquid samples

	This method (mM)			Commercial glucose meter (mM)		
Samples ($n = 3$)	Found	Mean	RSD	Found	Mean	RSD
Blood sample	4.81	5.11	±7.6%	4.94	4.95	±3.6%
	5.32			5.02		
Glucose oral liquid	5.21	72.1	±6.4%	4.90	71.6	±4.7%
	74.2			71.6		
	72.1			72.4		
	69.9			70.9		

4 Conclusions

In summary, a sensitive, simple fabrication and cost-effective nonenzymatic glucose electrochemical sensor was developed with nickel sulfide and biochar *via* a facile one-step electrochemical deposition method. The NiS–NiS_2/sludge-based biochar/GCE presented much better performance toward electrochemical nonenzymatic glucose sensing, higher selectivity for seven kinds of interferences (AA, DA, UA, Cys, NaCl, Mg^{2+} and Ca^{2+}), faster response (within 6 s), more highly reproducible, and long-term stability, than $Ni(OH)_2$–NiS_2/sludge-biochar/GCE, and NiS_2/biochar/GCE and even nonenzymatic sensor based on nickel sulfide in previews research. The excellent electrocatalytic properties toward glucose on NiS– NiS_2/sludge-based biochar/GCE mainly attributed to the synergistic effects of NiS–NiS_2 with electrocatalytical activity and biochar of multiple porous, abundant surface functional groups. Significantly, this study not only supplies a typical example of sewage sludge resource disposal but also suggests its potential to develop nonenzymatic electrochemical sensors based on NiS and NiS_2 in the future.

Author contributions

Conceptualization, Suxing Luo; methodology, Suxing Luo; validation, Meizhi Yang; writing—original draft preparation, Suxing Luo and Yuanhui Wu; writing—review and editing, Meizhi Yang and Jiang Li; supervision, Jiang Li; project administration, Yuanhui Wu; funding acquisition, Yuanhui Wu.

Conflicts of interest

The authors declare no conflict of interest.

Acknowledgements

This work was supported by the Guizhou Provincial Science and Technology Projects (Qian Kehe Jichu (2022) normal 573), the Zunyi Science and Technology Program Project (No. HZ [2021] 198 and No. Zunshikehe HZ[2022]136), the Special Key Laboratory of Electrochemistry for Materials of Guizhou Province

(No. QJHKYZ [2018]004),and the National Natural Science Foundation of China (No. 22166011).

References

1 X. Wang, E. Liu and X. Zhang, *Electrochim. Acta*, 2014, **130**, 253–260.
2 B. G. Amin, J. Masud and M. Nath, *J. Mater. Chem. B.*, 2019, **7**, 2338–2348.
3 Y. Zhuo, Y.-Q. Chai, R. Yuan, L. Mao, Y.-L. Yuan and J. Han, *Biosens. Bioelectron.*, 2011, **26**, 3838–3844.
4 M. L. Chelaghmia, M. Nacef, A. M. Affoune, M. Pontié and T. Derabla, *Electroanalysis*, 2018, **30**, 1117–1124.
5 B. Long, Y. Zhao, P. Cao, W. Wei, Y. Mo, J. Liu, C.-J. Sun, X. Guo, C. Shan and M.-H. Zeng, *Anal. Chem.*, 2022, **94**, 1919–1924.
6 S. Vinoth, P. M. Rajaitha, A. Venkadesh, K. S. Devi, S. Radhakrishnan and A. Pandikumar, *Nanoscale Adv.*, 2020, **2**, 4242–4250.
7 R. Qin, L. Hao, Q. Liu, J. Ju and Z. Qi, *Inorg. Nano-Met. Chem.*, 2021, 1–8.
8 J. C. Claussen, A. Kumar, D. B. Jaroch, M. H. Khawaja, A. B. Hibbard, D. M. Porterfield and T. S. Fisher, *Adv. Funct. Mater.*, 2012, **22**, 3399–3405.
9 Z. Ren, H. Mao, H. Luo, X. Deng and Y. Liu, *Nanotechnology*, 2020, **31**, 185501.
10 Y. Mu, D. Jia, Y. He, Y. Miao and H.-L. Wu, *Biosens. Bioelectron.*, 2011, **26**, 2948–2952.
11 N. Pal, S. Banerjee and A. Bhaumik, *J. Colloid Interface Sci.*, 2018, **516**, 121–127.
12 X.-m. Chen, Z.-j. Lin, D.-J. Chen, T.-t. Jia, Z.-m. Cai, X.-r. Wang, X. Chen, G.-n. Chen and M. Oyama, *Biosens. Bioelectron.*, 2010, **25**, 1803–1808.
13 T.-W. Lin, C.-J. Liu and C.-S. Dai, *Appl. Catal. B: Environ.*, 2014, **154**, 213–220.
14 H. Mao, Z. Cao, X. Guo, D. Sun, D. Liu, S. Wu, Y. Zhang and X.-M. Song, *ACS Appl. Mater. Interfaces*, 2019, **11**, 10153–10162.
15 S.-J. Yuan and X.-H. Dai, *Environ. Sci. Nano*, 2017, **4**, 17–26.
16 Z. Feng, R. Yuan, F. Wang, Z. Chen, B. Zhou and H. Chen, *Sci. Total Environ.*, 2021, **765**, 142673.
17 C. Kalinke, A. P. Zanicoski-Moscardi, P. R. de Oliveira, A. S. Mangrich, L. H. Marcolino-Junior and M. F. Bergamini, *Microchem. J.*, 2020, **159**, 105380.
18 G. A. Oliveira, A. Gevaerd, A. S. Mangrich, L. H. Marcolino-Junior and M. F. Bergamini, *Microchem. J.*, 2021, **165**, 106114.
19 M. V. Sant'Anna, S. W. Carvalho, A. Gevaerd, J. O. Silva, E. Santos, I. S. Carregosa, A. Wisniewski Jr, L. H. Marcolino-Junior, M. F. Bergamini and E. M. Sussuchi, *Talanta*, 2020, **220**, 121334.
20 P. R. de Oliveira, C. Kalinke, J. L. Gogola, A. S. Mangrich, L. H. M. Junior and M. F. Bergamini, *J. Electroanal. Chem.*, 2017, **799**, 602–608.
21 K. Nan, H. Du, L. Su and C. M. Li, *ChemistrySelect*, 2018, **3**, 7081–7088.
22 M. Dong, Z. Chai, J. Li and Z. Wang, *Ionics*, 2020, **26**, 4095–4102.
23 Y. Ma, M. Li, P. Li, L. Yang, L. Wu, F. Gao, X. Qi and Z. Zhang, *Bioresour. Technol.*, 2021, **319**, 124199.
24 X. Li, K. Liu, Z. Liu, Z. Wang, B. Li and D. Zhang, *Electrochim. Acta*, 2017, **240**, 43–52.
25 R. Sakthivel, A. Geetha, B. Anandh, S. Mohankumar and J. Dineshkumar, *J. Mater. Sci.: Mater. Electron.*, 2022, 1–14.
26 D. Wu, X. Xie, J. Zhang, Y. Ma, C. Hou, X. Sun, X. Yang, Y. Zhang, H. Kimura and W. Du, *Chem. Eng. J.*, 2022, 137262.
27 B. Qiu, Y. Zhang, X. Guo, Y. Ma, M. Du, J. Fan, Y. Zhu, Z. Zeng and Y. Chai, *J. Mater. Chem. A*, 2022, **10**, 719–725.
28 N. Yang, C. Tang, K. Wang, G. Du, A. M. Asiri and X. Sun, *Nano Res.*, 2016, **9**, 3346–3354.
29 K. Xia, Y. Cong, Y. Chen, L. Tian, Y. Su, J. Wang and L. Li, *Sens. Actuators, B*, 2017, **240**, 979–987.
30 S. Luo, M. Yang, Y. Wu, J. Li, J. Qin and F. Feng, *Micromachines*, 2022, **13**, 115.
31 C.-Y. Ko, J.-H. Huang, S. Raina and W. P. Kang, *Analyst*, 2013, **138**, 3201–3208.
32 Z. Ren, H. Mao, H. Luo and Y. Liu, *Carbon*, 2019, **149**, 609–617.
33 S. Wang, L. Zhang, Y. Tian, L. Lin and S. Zhuiykov, *J. Electrochem. Soc.*, 2019, **166**, B1732.
34 S. Kim, S. H. Lee, M. Cho and Y. Lee, *Biosens. Bioelectron.*, 2016, **85**, 587–595.
35 S. Radhakrishnan and S. J. Kim, *RSC Adv.*, 2015, **5**, 44346–44352.
36 R. Singh and M. M. Ayyub, *ACS Appl. Electron. Mater.*, 2021, **3**, 1912–1919.
37 H. Huo, Y. Zhao and C. Xu, *J. Mater. Chem. A*, 2014, **2**, 15111–15117.